Biomedical Signal Processing and Control 87 (2024) 105479

Contents lists available at ScienceDirect

Biomedical Signal Processing and Control

journal homepage: www.elsevier.com/locate/bspc

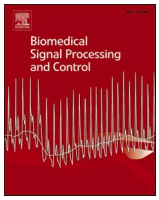

Blood pressure monitoring with piezoelectric bed sensor systems

Xiaoman Xing [a,b,*], Huan Li [c], Qi Chen [c], Chenyu Jiang [d], Wen-fei Dong [b,e,*]

[a] School of Biomedical Engineering (Suzhou), Division of Life Sciences and Medicine, University of Science and Technology of China, Suzhou, Jiangsu, China
[b] Suzhou Institute of Biomedical Engineering and Technology, Chinese Academy of Sciences, Suzhou, Jiangsu, China
[c] Beijing Anzhen Hospital, Capital Medical University, Beijing Institute of Heart, Lung and Blood Vessel Diseases, Beijing, China
[d] Jinan Guoke Medical Technology Development Co., Ltd., Jinan, Shandong, China
[e] Suzhou GK Medtech Science and Technology Development (Group) Co. Ltd, Suzhou, Jiangsu, China

ARTICLE INFO

Keywords:
Ballistocardiography
Blood pressure
Bed-sensor system
Higuchi fractal dimension
Transfer learning

ABSTRACT

Objective: Ballistocardiography (BCG) measures vital signals without direct contact, which shows great potential for continuous sleep monitoring. This study proposed a BCG-based blood pressure (BP) estimation algorithm framework using piezoelectric bed sensor systems. **Methods:** To derive BP, a combination of morphological features, spectral features, and fractal dimensions of the BCG signal were utilized. Bayesian neural networks were employed to weigh the contribution of each feature and generate input-dependent coefficients. Two data balancing procedures were tested, and the proposed system's effectiveness was evaluated, including in-hospital patients and healthy subjects. Transfer learning techniques were employed to further improve the system's performance and showcase the similarity between bed systems with different piezoelectric sensors. **Results:** The combination of morphological and spectral features significantly improves BP estimation accuracy. The fractal dimension captures short-term BP fluctuations, improving intra-subject BP trend estimation. For young and healthy subjects, calibration-free mean absolute error (MAE) for systolic BP (SBP) and diastolic BP (DBP) is 4.20/4.25 mmHg at a 5-second time resolution. In the case of in-hospital patients, the best MAE for overnight SBP/DBP is 9.96/7.59 mmHg. Transfer learning, combined with data balancing techniques, substantially enhances BP estimation accuracy for in-hospital patients, providing insights for future algorithm designs. **Conclusion**: The study concludes that bed-sensor systems can track BP changes in relatively healthy subjects. However, BCG alone may not be sufficient for subjects with severe cardiovascular dysfunctions to obtain reliable BP readings. Transfer learning and proper data balancing may facilitate the fast development of new bed sensor systems with similar technologies.

1. Introduction

Hypertension is associated with multiple vascular injuries, which may lead to poor prognosis. Its early prevention and control are of great significance. Ambulatory blood pressure (BP) measurement leads to better diagnosis and management of hypertension, and nocturnal BP is a more sensitive cardiovascular prognostic indicator than daytime or 24-hour mean BP [1–5]. Under normal circumstances, due to the excitation of parasympathetic nerves at night, BP should be lower than during the daytime, forming a dipper pattern. However, in disease conditions, the circadian rhythm may change, and sympathetic excitation at night forms a non-dipper pattern, leading to the deterioration of cardiovascular diseases. A recent study published in Lancet highlighted the informative nature of nighttime systolic blood pressure (SBP) regarding the risk of all-cause death and cardiovascular death [4]. Continuous BP monitoring during sleep can also help reveal the etiology of masked hypertension and resistant hypertension, which could assist in the management of metabolic diseases [6–9].

Currently, cuff sphygmomanometers are commonly used as ambulatory blood pressure monitors. However, the process of inflation and deflation is intrusive and can disturb sleep, potentially leading to false perceptions of nocturnal BP. The sampling rate is also low, with only about 10–30 data points per night, making it difficult to obtain detailed BP fluctuations. Additionally, the high price and tedious preparation work make it unsuitable for daily monitoring in the home setting. As a result, many research institutions and manufacturers have turned to innovative wearable or non-contact BP estimation technologies in recent years. The most popular ones are the volume clamp method [10],

* Corresponding authors.
E-mail addresses: xingxm@sibet.ac.cn (X. Xing), wenfeidong@126.com (W.-f. Dong).

https://doi.org/10.1016/j.bspc.2023.105479
Received 1 December 2022; Received in revised form 15 August 2023; Accepted 12 September 2023
Available online 16 September 2023

tonometry [11], photoplethysmography (PPG) [12], and ballistocardiography (BCG)-based BP estimation technologies [13]. Among them, BCG was the least intrusive, as it could be deployed in a non-contact form without any limitations on device size or battery life. The sensing system could also be turned on automatically every night, making it convenient for end-users [14].

BCG originates from the tiny vibration of the body caused by the heartbeat. Compared with PPG, it does not need force-volume conversion, which can effectively retain its high-frequency information. The anti-interference ability and repeatability of accelerometers are also stronger than optical sensors [15]. Therefore, BCG may be a more suitable modality for measuring BP. The theory of BCG-based BP estimation has been developed for several years [16–18]. For example, Kim *et al.* obtained the standard BCG waveform by simulating aortic blood flow and the biomechanics of the human body [17,18]. Yousefian *et al.* used a similar approach and obtained the sensitivity of BCG waveforms to cardiovascular properties [16]. Guidoboni *et al.* extended the theoretical framework and incorporated hemodynamics in the BCG simulation [19]. With the progress of theoretical studies, multiple attempts have been tried to develop a BCG-BP system.

BCG can be measured using different sensor systems [20,21]. Some of the representative studies were shown in Table 1. For BP estimation, three main device setups were used. The first setup involved using a weighing scale that measured the BCG force perpendicular to the device's surface [17,18,22]. While the signal obtained from the scale was strong and had less interference, it was not suitable for continuous long-term monitoring of BP. The second approach involved utilizing accelerometers, primarily worn on the wrist, which measured seismography (SCG), a derivative form of BCG [16,23–25]. This wearable device had substantial potential for continuous BP monitoring. However, the accuracy of SCG was highly dependent on posture, making it difficult to standardize the algorithm. The third and most convenient setup involved using a bed sensor system, which could use piezoelectric, hydraulic, or optical techniques [13,26,27]. Most of the bed sensor systems were used to estimate heartrate and respiratory rate, instead of BP [28–31]. In this study, we investigated two piezoelectric bed systems with similar but different sensing technologies and evaluated the transferability of the algorithm.

Studies found that different BCG measurement systems may be used to evaluate cardiovascular parameters and BP. Yao *et al.* found that BCG morphological features correlated with BP, stroke volume (SV) and total peripheral resistance (TPR) [32]. Martin *et al.* found that BCG-derived pulse transition time (PTT) was more accurate and correlated with BP compared to PPG derived PTT when weighing scales were used [22]. Kim *et al.* found that the association of BCG features and BP was stronger than PPG in most cases, but inferior in others [17,18]. Yousefian *et al.* measured wrist SCG, which achieved a mean absolute error (MAE) of 8.3 $\pm$ 0.7 mmHg for SBP and 6.0 $\pm$ 0.5 mmHg for diastolic BP (DBP) with a linear fitting algorithm [23]. If BCG data were combined with PPG, the MAE of SBP and DBP estimation could be further reduced [25]. The waveform of the supine BCG is significantly different from that of the standing and seated positions [36–38]. Su *et al.* used a hydraulic sensor system with a bed sensor setup and found a linear correlation of BCG amplitude and BP in healthy subjects [13]. Carlson *et al.* established a complete BCG-vitals dataset, and reported a high correlation between BCG and vital signs such as BP and SV [26].

There were two main issues with the current BCG-BP studies. One is the lack of diversity in study populations. Previous studies predominantly used young and healthy subjects to establish BCG-BP models, which might be ineffective in subjects with hypertension or comorbidities. Another is the transferability of the algorithm. Although BCG measured by different devices may be translatable from one to another, its equivalence in BP estimation was not thoroughly evaluated [32,39]. To address these issues, we studied subjects with diverse age and health status. Additionally, the potential equivalence of piezoelectric-sensor bed systems was evaluated by transferring the algorithm from one dataset to another. This approach enables the efficient training of a new model with a similar bed-sensor system.

To sum up, our objective was to investigate the accuracy of BP estimation from supine BCG measured by piezoelectric bed sensors. Key findings include:

(1) A novel two-step spectral analysis technique was developed by combining wavelet and Fourier transformations, which captured both high-frequency morphological details and non-stationary fluctuations of BCG. This method was robust in the presence of environmental disturbances, allowing for improved BP estimation accuracy.
(2) Spectral and morphological features complemented each other and should be combined to achieve better regression results.
(3) Higuchi fractal dimension (HFD) was found to be informative in describing the overlap of residual vibrations from central blood flow momentum. HFD was less affected by noise and contained more information about short-term BP fluctuation.
(4) The implementation of data balancing techniques contributes to enhanced BP estimation performance, although careful consideration should be given when selecting the balancing procedure.
(5) The BCG-BP algorithm can be transferred from one bed sensor system to another with similar sensing technology. The pre-trained neural network significantly improved BP estimation in smaller datasets.
(6) The accuracy of BP estimation derived from piezoelectric bed sensors may decrease with the presence of cardiovascular diseases.

The remainder of this paper is organized as follows: Section 2

Table 1
Representative studies on BCG-based BP estimation.

Sensor type	Protocol	Representative studies	Pros	Cons
Weighing scale (Force)	Standing + interventions (cold press, mental arithmetic, slow breathing, breath holding, stair climbing, etc.)	Kim *et al.* [17,18]; Martin *et al.* [22] Yao *et al.* [32] Shin *et al.* [33,34]	1.Stronger signal; 2.Standardized posture; 3.Convenient for snapshot BP measurement.	1.Not suitable for continuous long-term monitoring; 2. Specialized equipment is needed.
Wrist watch/Armband (Accelerometer)	Same as weighing scale	Yousefian *et al.* [16,23–25] Yao *et al.* [32]	1.Convenient for continuous BP measurement; 2. Implantable to existing smart watches; 3. Translatable to weighing-scale BCG.	1.Weaker signal at limbs; 2.Posture dependent; 3.Motion artifact; 4.Good contact is needed.
Ear worn (Accelerometer)	Standing, tilt maneuvers	He *et al.* [35]	1. Daytime continuous monitoring; 2. Combination of multiple sensors with pre-ejection (PEP) estimation.	1. Posture dependent; 2. Low signal-to-noise ratio; 3. Good contact is needed; 4. High faulty PEP measurement rate.
Bed sensor (Hydraulic)	Supine (6–10 min)	Su *et al.* [13]	1.Overnight monitoring; 2. Respiratory measurement; 3. Acquire pulse transition time without wearing multiple sensors.	1. Weaker BCG signal; 2. Signals affected by the mechanical properties of the bed and its components, such as the mattress and bed frame; 3. Posture-dependent.
Bed sensor (Electromechanical)	Supine (~5 min)	Carlson *et al.* [26]		

describes the BCG data collection and processing procedures. This includes a discussion of feature combination, data balancing, the construction of Bayesian neural networks (BNN), and transfer learning from a larger database. Section 3 presents the results of BP estimation using BNN, including an ablation analysis of feature combinations and preprocessing steps. It also encompasses an analysis of the performance improvement achieved through transfer learning. Section 4 discusses the implications of our findings and helps to define the scope of application for BCG-based BP estimation via a bed-sensor system. Finally, Section 5 concludes the paper.

2. Method

This section describes the data collection and processing procedures used for two datasets. Along with conventional BCG morphological features, a two-step spectral analysis was utilized to incorporate additional information. HFD was chosen as a critical descriptor for estimating short-term BP fluctuation. Furthermore, we offer a comprehensive description of the data-balancing techniques and the procedures in transfer learning.

2.1. Dataset description

The BCG-BP datasets were from two different bed sensor systems, hereby denoted as dataset-SIBET and dataset-KSU. Dataset-SIBET was collected by our team in Capital Medical University Affiliated Anzhen Hospital. Subjects with severe cardiovascular dysfunctions and sleep disorders were recruited. BCG signals were acquired by piezoelectric-ceramic sensors and BP was obtained by ambulatory cuff sphygmomanometers. Dataset-KSU was shared by Carlson *et al.* [26], which consists of short BCG-BP measurements from 40 young and healthy subjects. BCG signals were acquired with electromechanical films (EMFi) sensors and beat-to-beat BP references were obtained from Finapres Medical Systems. Although these sensors were built with different materials, they were both piezoelectric, which means that their working principals were similar. The only difference would be the sensitivity and temporal response curve. The algorithm developed with these two sensors may be transferrable with feature adaptation.

2.1.1. Dataset-SIBET

For dataset-SIBET, ten piezoelectric-ceramic sensors (Yueyang Medical Ltd.) were used to measure BCG at the neck and chest sites. Piezoelectric ceramics are generally stiffer and more brittle than EMFi sensors [20,40]. They have a higher piezoelectric effect coefficient and can generate a higher electrical output voltage than EMFi sensors [31]. Sensors were positioned in two rows and sealed in a waterproof cover, which was placed under the mattress. Five sensors were under the pillow and five were under the chest, as shown in Fig. 1. BCG data from the neck side were summed to reduce the fluctuation caused by the neck position. Signals from the chest side were mainly used to estimate the heart rate and respiration, which were added to the input feature set for the regression algorithm. Due to strong interference from respiration, we didn't use morphological or spectral features of chest signals to estimate BP. This study was approved by the ethics committee of the Capital Medical University Affiliated Anzhen Hospital (IRB 2020074X), which conforms to the principles outlined in the Declaration of Helsinki.

Dataset-SIBET includes overnight recordings obtained from 28 in-hospital participants who underwent overnight BP measurements. Table 2 provides a detailed breakdown of participant demographics. Hypertension, diabetes, stroke, kidney disease, and hyperlipidemia were among the health conditions of the participants, and many had multiple conditions simultaneously. The complete list of the health conditions of the subjects were shown in Supplementary Table 1. Participants were instructed to lie on the mattress with their necks comfortably rested on the pillow, with no discomfort or constraints. Brachial BP measurements were captured by an ambulatory blood pressure monitor (A&D, TM-2430) at 20-minute intervals, while BCG signals were continuously sampled at 50 Hz and transmitted to a cloud-based database. A total of 657 BP measurements were obtained.

Recruiting female subjects with both sleep disorders and severe cardiovascular diseases proved challenging, leading to a sex imbalance in the study. For traditional cuff sphygmomanometers, biological sex is not a required input. Previous studies have shown no significant correlation between sex and pulse wave velocity [41–43]. BCG is a mechanical signal that is primarily influenced by biometric factors such as height, weight, and age, with sex representing an implicit influence rather than an explicit one. As a result, our algorithm was developed without considering sex as an input.

2.1.2. Dataset-KSU

Dataset-KSU used a different bed system [26,44,45]. Four electromechanical films (EMFit; L series; 300 mmx580 mm) were employed to obtain BCG readings from study participants, as illustrated in Fig. 2. While their piezoelectric effect was lower compared to ceramics, their response to pressure or force was still rapid and linear, implying that the two bed sensor systems were likely to be equivalent for BP estimation purposes. Beat-to-beat BP references were obtained from Finometer PRO. Raw BCG data were sampled at a 1 kHz rate, which was down-sampled to 100 Hz and bandpass-filtered between 0.1 and 24 Hz. In this study, data from Film 0 was used due to its higher signal quality,

Table 2
Participant demographics.

	Dataset-SIBET	Dataset-KSU
Num of Subjects	28	40
Age (years)	45.3 ± 11.5*	33.9 ± 14.5
Height (cm)	174.1 ± 6.8	171.1 ± 10.7
Weight (kg)	90.6 ± 13.1*	76.0 ± 17.6
BMI (kg/m^2)	29.6 ± 3.9*	26.0 ± 5.7
Sex(M/F)	26/2	17/23
SBP (mmHg)	145.7 ± 25.4*	120.3 ± 14.0
DBP (mmHg)	88.4 ± 17.8*	69.5 ± 13.0

* Significantly different compared to Dataset-KSU. The two-sample *t*-test was used. BMI: body mass index.

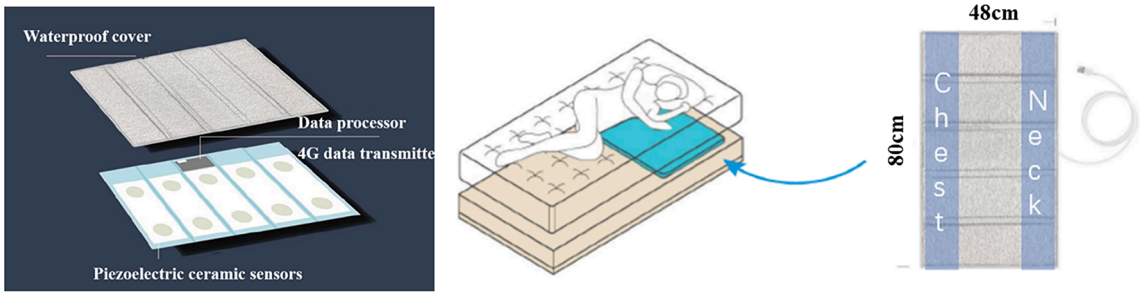

Fig. 1. Design of a multi-point-sensor system.

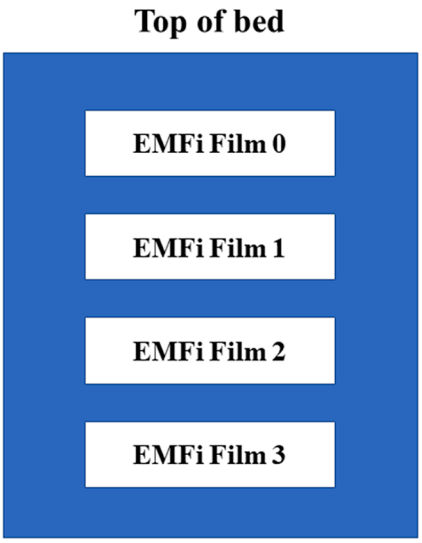

Fig. 2. Design of a multi-strip-sensor system.

which corresponds to the neck sensor in dataset-SIBET. A total of 17,577 BP measurements were collected.

2.2. Feature extraction

For dataset-KSU, BCG signals and BP were simultaneously and continually recorded. The finger cuff from the Finometer device was considered to have negligible interference with BCG signals as it exerted minimal force on the finger. Reference systolic and diastolic blood pressure were determined for each cardiac cycle by measuring corresponding peaks. The KSU data was segmented into 5-second windows to facilitate reliable respiration estimation, with BP and morphological features averaged in each window to create a predictor-response pair as depicted in Fig. 3a. A leave-one-subject-out partition scheme was utilized to avoid contamination of training and testing data. For dataset-SIBET, BP references were obtained using a cuff sphygmomanometer, with BCG data from the 60 s preceding inflation. A sliding window of 5 s was utilized to calculate the variation of characteristic peaks, and the window with the smallest variation was chosen to predict BP, as shown in Fig. 3b. Any measurement in either dataset with a standard deviation of I or J peaks higher than 30% of the mean value or consecutive DBP change more significant than 10 mmHg for dataset-KSU was excluded, resulting in a total of 14,468 measurements for dataset-KSU and 552 measurements for dataset-SIBET.

2.2.1. Morphological feature extraction

Most of the previous studies used morphological features to estimate BP [13,17,26]. Features such as I, J, K, and L peaks, as shown in Fig. 3a, and the intervals in-between were used to build a BCG-BP model. The advantage of using morphological features is that the physiological meaning of each peak could be explained. For example, the onsets of aortic inlet and outlet BP waves roughly correspond to the initiation of the I wave and the peak of the J wave [18]. However, these features were prone to environmental disturbances, and the information contained by individual features was limited.

2.2.2. Spectral feature extraction

The transmission of vibration throughout the body was found to be frequency-dependent [46–48]. For BCG segments, we performed a continuous 1D wavelet transformation using Morlet wavelet kernels,

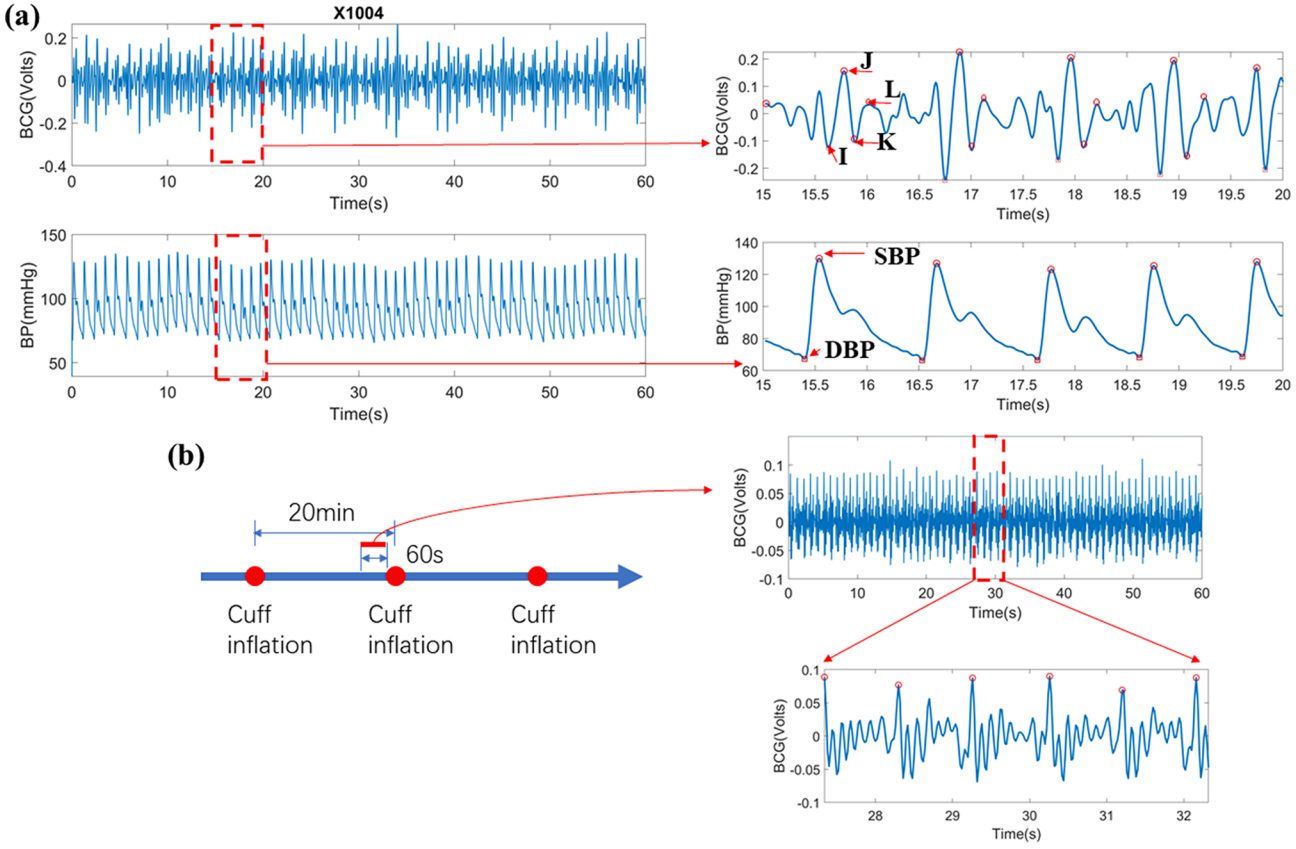

Fig. 3. Signal selection procedure. (a) Continuous acquisition from dataset-KSU. The locations of characteristic peaks such as I, J, K, and L were labeled. (b) Intermittent signal acquisition and selection from dataset-SIBET, a five-second segment was chosen before the cuff inflation.

followed by a Fourier transformation of each spectral component (amplitude) to extract longer-term frequency-domain fluctuations. So that the frequency-time representation of the signal (as shown in Fig. 4B) was replaced by a frequency-frequency representation (as shown in Fig. 4C). A detailed illustration of this two-step spectral analysis is provided in Fig. 4, yielding a 2D spectrum with both high-frequency details and long-term periodicity [20,49,50].

The center frequency of the Fourier transformation (f_0) was different for each measurement, which should be around the heart rate. We standardized the spectral image by selecting the Fourier frequency range of f_0-0.25 Hz to $f_0 + 0.25$ Hz and wavelet frequency of 2 to 14 Hz.

To reduce redundant information, we compressed the spectrum showcased in Fig. 4C by reshaping the 2D matrix into a 1D array and applying singular value decomposition (SVD). The first 6 most important components were calculated per dataset, which were then reshaped back into a 2D spectrum and illustrated in Fig. 5 (dataset-SIBET) and supplementary Figure S1(dataset-KSU). As pointed out by Yao *et al.*, the most important harmonics may contain the majority of the information [47]. The first 6 components explained 91.4% of the variation in dataset-KSU and 87.9% of the variation in dataset-SIBET. One interesting observation was that the first and second components explained 61.0% and 12.3% of the variation in dataset-KSU, while the corresponding numbers in dataset-SIBET were 67.3% and 7.4%. One possible explanation was the increased heterogeneity in cardiovascular activity for in-hospital patients.

2.2.3. Higuchi fractal dimension (HFD)

Human bodies could be mechanically modeled as a combination of springs and dampers. Each heartbeat happens with varying strength and timing, which leads to body and limb vibrations with different time scales. The fractal dimension could be used to estimate the chaotic pattern caused by the vibration propagation through the cardiovascular tree. HFD of the BCG wavelet component was calculated as shown in the Appendix.

2.2.4. Other features

Biometric features, heart rate, and respiration were added to ensure the completeness of the feature information.

2.2.4.1. Biometric information. To build a BCG-BP model, biometric information such as age, weight, and height was used. Age mainly influences vascular stiffness, which has a non-neglectable effect on aortic blood pressure and blood flow velocity. If human bodies are modeled as distributed weights with connecting springs and dampers, the transfer function from central blood pressure to body motion becomes highly personal. Both body weight and height were needed to estimate the transfer function.

We found that age was significantly correlated with SBP for dataset-KSU, as shown in Table 3. In comparison, age had no correlation with SBP or DBP for dataset-SIBET or diseased subjects. The correlation between weight and BP was smaller for dataset-SIBET, indicating irregular vibration signal transfer.

2.2.4.2. Respiration and heart rate. Respiration modulates the lower frequency (0.2–0.6 Hz) in BCG signal and BP fluctuation. The BCG signal was passed through a Butterworth bandpass filter with cut-off frequencies at 0.1 Hz and 0.5 Hz [51]. Advanced peak detection algorithms were used to reduce the influence of environmental disturbances. Since we didn't need beat-to-beat heart rate, we used the dominant frequency f_0 to calculate heart rate, as described in section 2.2.2 and shown in Fig. 4.

2.3. Data balancing and the feature combination scheme

If the measurement data were severely unbalanced, the learned algorithm would focus on reducing the errors around the median BP, which resulted in less discriminative power. To address this issue and enhance BP estimation accuracy, we employed two EasyEnsemble procedures [52]. The first procedure aimed to create a balanced distribution of BP values. We divided SBP readings between 85 mmHg and 200 mmHg into bins of 5 mmHg. For DBP, the range was 55 mmHg to 100 mmHg. Within each bin, an equal number of samples were randomly selected without replacement to ensure balance. The second procedure sought to generate a balanced distribution of relative BP changes compared to a baseline measurement (ΔBP). The baseline was established by averaging the first 5 measurements for dataset-KSU and first 2 measurements for dataset-SIBET. Subsequent BP readings were resampled to create an evenly distributed ΔBP range spanning from −50 mmHg to 50 mmHg, with a step size of 5 mmHg. If the number of samples in a bin was insufficient, all available samples were included. These balanced datasets were then utilized for training the regression algorithm and evaluating the testing data. It is worth noting that the testing data did not require balancing. Multiple resampling iterations were performed, and the resulting algorithms were averaged to enhance

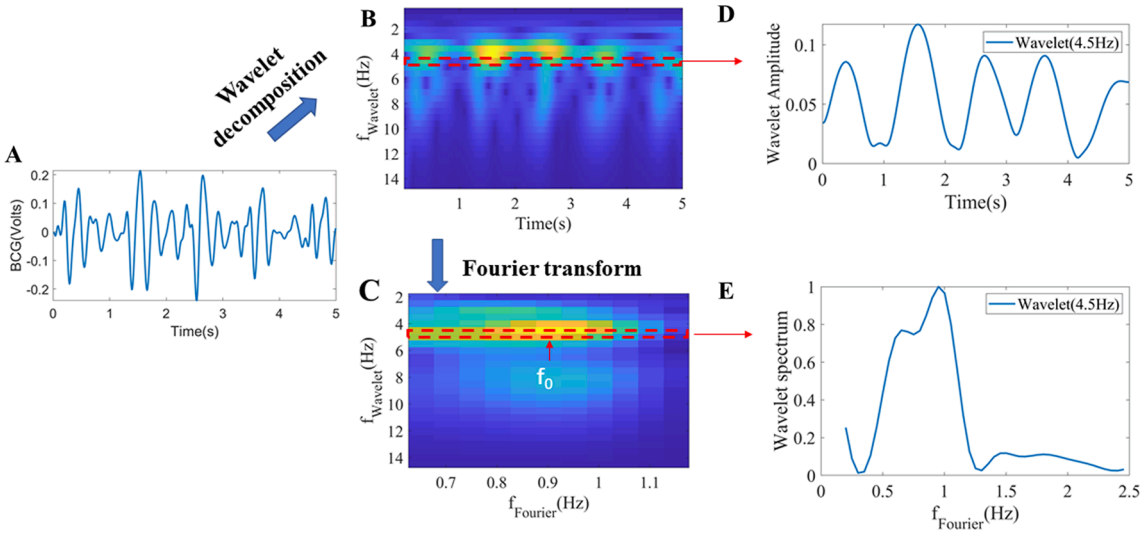

Fig. 4. Spectral analysis procedure. (A) Step 1: Original BCG signal. (B) Step 2: Wavelet decomposition using Morlet wavelet kernels. (C) Step 3: Fourier transformation of each wavelet component. (D) Individual wavelet component (4.5 Hz) from subplot B. (E) Spectrum of the individual wavelet component (4.5 Hz) from subplot C.

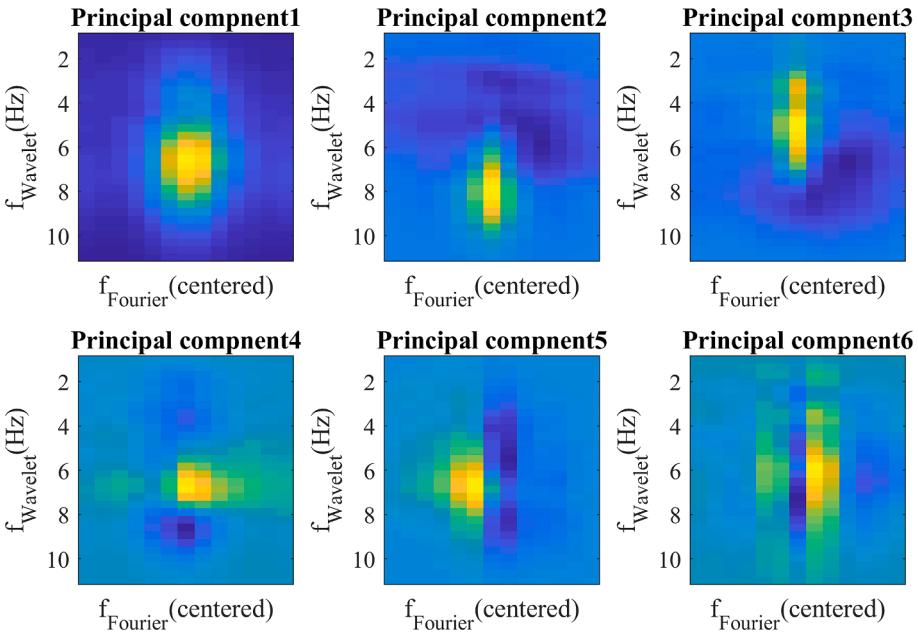

Fig. 5. Principal components of the 2D spectrum(dataset-SIBET).

Table 3
Pearson correlation coefficients (r) of biometrics and BP.

Biometrics	Dataset-KSU		Dataset-SIBET	
	SBP	DBP	SBP	DBP
Age	0.44*	0.02	−0.05	−0.06
Weight	0.41*	0.26*	0.17*	0.14*
Height	0.16*	0.10*	0.16*	0.13*

* significant correlation between a biometric feature and SBP/DBP.

their robustness. Furthermore, it is crucial to acknowledge that the proposed ΔBP procedure does not completely address the issue of ΔBP imbalance. The combination of multiple ΔBP leads to a new ΔBP based on the selected starting baseline and the time interval in between. The impact of these factors on algorithm performance is contingent upon the distribution of the data [53].

Feature selection was also important for BP estimation. In this study, the focus was not on individual features. Instead, we tested groups of features, so that enough relevant information could be obtained. We compared several feature combination schemes and the best was chosen to produce the final algorithm.

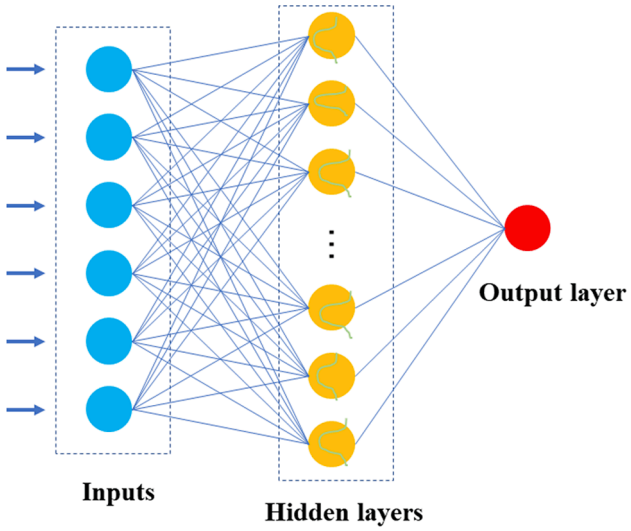

Fig. 6. Bayesian neural network.

2.4. Bayesian neural network (BNN)

To estimate BP using selected features as inputs, we chose to use the Bayesian neural network, as illustrated in Fig. 6. Fleischhauer *et al.* reported that the feature contribution to the target was different depending on the query point [54]. Bayesian optimization enabled us to apply a probability distribution over possible neural networks, mitigating overfitting problems and making it more suitable for algorithms with input-dependent coefficients. Independent BNNs were initially trained for both datasets. We then used the network coefficient from dataset-KSU as a starting point to improve BP estimation for dataset-SIBET.

The algorithm's performance was evaluated using mean absolute errors (MAE) of BP and intra-subject BP fluctuation relative to baseline (ΔSBP and ΔDBP), measuring both inter-subject and intra-subject correlations between prediction and ground truth. For dataset-KSU, the first five data points were averaged to derive a calibration factor, while for dataset-SIBET, the first two data points were used as there were fewer measurements per subject. These calibration data points were added to the training process to adjust the coefficients within the model. Additionally, the calibration factor was subtracted from subsequent BP estimations to improve accuracy.

2.5. Transfer learning

Transfer learning involves transferring knowledge learned from a pre-trained model (source domain) to a new, similar but different task (target domain) [55,56]. For example, Jared Leitner *et al.* built a customized PPG-BP model with assistance from the large public databases(MIMIC III), and achieved improved results [57]. In this study, we adopted transfer learning technique due to two reasons. Firstly, several studies have also shown that BCG measured by different technologies were translatable from one to another [32,39,58]. Secondly, we had access to a large public database with comparable sensing technology, which made transfer learning less complex, particularly if we employed similar pre-processing steps. The process was demonstrated in Fig. 7.

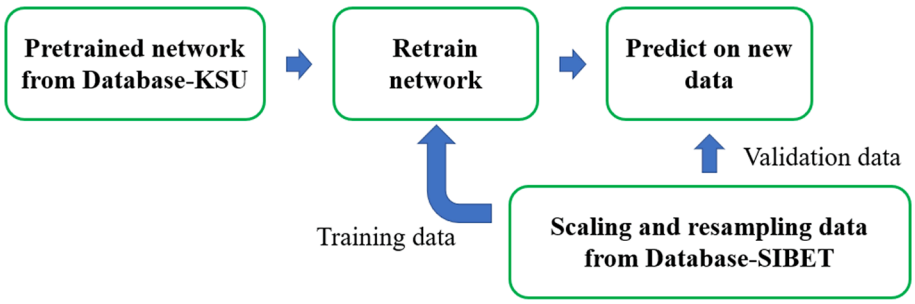

Fig. 7. Transferring knowledge from dataset-KSU to dataset-SIBET.

Analytical features obtained from ceramic sensors were scaled by amplitude to match the sensitivity of EMFi sensors, while frequency-domain features were resampled at 100 Hz. Rather than initiating BNN training with default coefficients, we leveraged the pre-trained BNN from dataset-KSU. Fine-tuning was conducted by gradually unfreezing the layers and adapting the weights to the new dataset. This approach enabled us to exploit the learned features of the pre-trained model to achieve better performance using much less labeled data in the target domain.

2.6. Ablation study

We conducted an ablation study to assess the significance of key preprocessing steps. Firstly, we examined the impact of data balancing by replacing the balanced data with randomly selected samples for each round of EasyEnsemble. Additionally, we compared the algorithm's performance using various pretrained models, balancing techniques and frequency-domain principal components for transfer learning. These ablation experiments aimed to provide insights into the role and significance of key preprocessing steps in our algorithm's performance.

3. Results

In this section, we performed BP estimation using different combinations of BCG features, data balancing techniques, and transfer learning approaches. To highlight the importance of preprocessing steps, we conducted ablation experiments to illustrate their impact on the overall model performance. The results of both independent estimation models and transfer-learning adjusted models for dataset-SIBET were carefully documented and evaluated.

3.1. Performance with different feature combinations

In order to evaluate the impact of different input feature combinations, a BNN structure consisting of one hidden layer with 15 neurons was utilized. It is essential to note that while this structure may not be optimized for practical deployment, its purpose was to directly compare performances resulting from various feature combinations. Leave one subject out partition scheme was used to make sure the training data and testing data were rigorously separated. Intra-subject correlation was calculated by comparing the ground truth and estimation of ΔBP. Both MAE and correlation coefficients were used to evaluate the performance of the algorithm. We assessed the algorithm's performance by comparing different feature combinations, which we have summarized in Table 4 and Supplementary Table 2. These findings provide valuable insights that improve our understanding of the significance of feature combinations within the context of this study.

For dataset-KSU, the combination of TD and FD had significantly better performance than TD or FD alone from all aspects, as expected. The addition of HFD significantly improved the intra-subject and overall BP correlation, which also reduced MAE of SBP with marginal significance. The combination of all features produced the best MAE and highest correlation. The contribution of features to BP estimation performance was exemplified in Fig. 8 and Supplementary Figure S4.

Table 4
Performance comparison for different feature combinations with BP balancing and no pretraining (SBP).

		FD	TD	FD + TD	FD + TD+HFD	FD + TD+HFD + Bios
Dataset-KSU	MAE of SBP estimation (mmHg)	6.13	7.18*	5.81*	4.99	4.20*
	MAE of ΔSBP estimation (mmHg)	7.19	7.11	6.70*	6.62	5.33*
	Intra-subject correlation	0.19	0.12	0.24*	0.38*	0.48*
	Overall SBP correlation	0.84	0.80	0.85*	0.89*	0.92*
Dataset-SIBET	MAE of SBP estimation (mmHg)	15.23	16.09	12.27*	10.67*	11.95
	MAE of ΔSBP estimation (mmHg)	13.44	13.45	13.40	12.82	15.12*
	Intra-subject correlation	0.20	0.05	0.23*	0.51*	0.49
	Overall SBP correlation	0.53	0.34*	0.61*	0.72	0.68

* significantly different from the left column. The MAE and intra-subject correlation comparison were done using a paired *t*-test. The *r* comparison was done by testing the significance of a non-zero correlation between the BP estimation difference across groups and ground truth.

For dataset-SIBET, the combination of TD and FD significantly improved the correlation coefficients and MAE. Adding biometrics didn't bring any benefit, except that the MAE of DBP and ΔDBP was slightly reduced, as shown in Supplementary Table 2. Interestingly, the best intra-subject DBP correlation in dataset-SIBET was higher than dataset-KSU, although the MAE of DBP or ΔDBP was higher. This might be caused by the fewer measurements and large ΔDBP range during several hours of sleep. The standard deviation of ΔDBP was 12.4 mmHg in dataset-SIBET, while the corresponding number in dataset-KSU was 5.3 mmHg.

We found that FD features were more stable. Interestingly, intra-subject SBP correlation was improved by the addition of biometrics, due to the overall better quantification of biomechanical properties. Similar trends were observed with DBP, with the addition of HFD resulting in significant improvement across all aspects of DBP estimation. However, the inclusion of biometrics only led to slight enhancements in DBP estimation performance, as demonstrated in Supplementary Table 2.

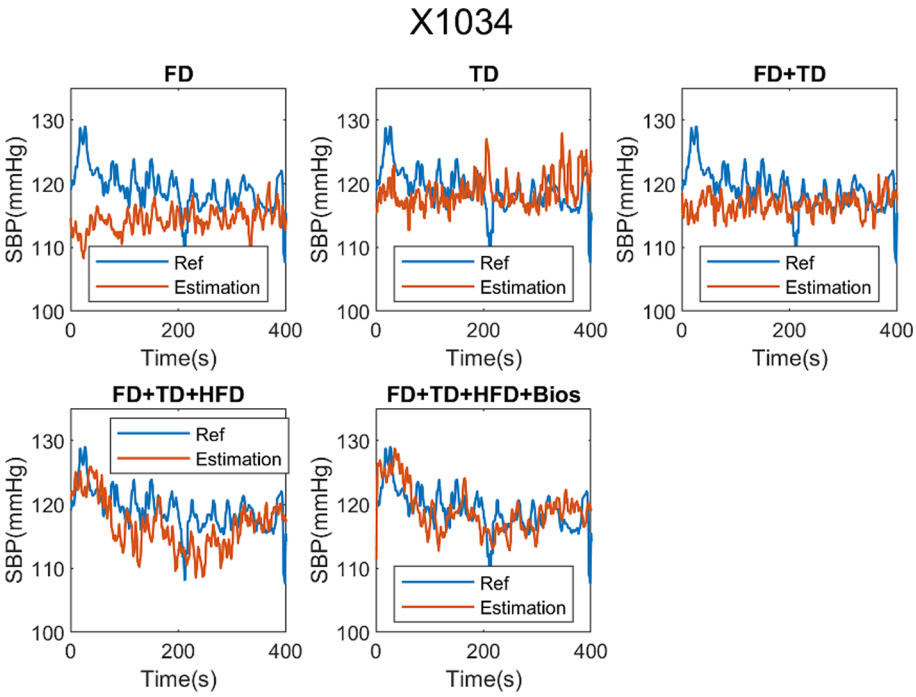

Fig. 8. Example of SBP estimation with different feature combinations (dataset-KSU).

3.2. Importance of data-balancing before training

Training a model on a severely unbalanced dataset can potentially lead to poor generalization performance as it fails to capture the underlying features of the minority class. However, the impact of data balancing on performance improvement is not always straightforward and can sometimes even degrade performance [53]. Our findings indicate that for dataset-KSU, BP balancing yielded slightly better results, as shown in Table 5, while ΔBP balancing had a detrimental effect on performance. Surprisingly, for dataset-SIBET, both balanced ΔBP and BP significantly enhanced MAE and overall correlation of SBP. While the exact reason remains uncertain, one possible explanation is that ΔBP balancing works better when dealing with measurements featuring higher BP fluctuation. In dataset-KSU, where beat-to-beat measurements resulted in much smaller ΔBP and ΔBP variation, ΔBP balancing was less advantageous. Conversely, in dataset-SIBET, ΔBP balancing also led to a more balanced BP compared to unbalanced data. This suggests that multi-dimensional balancing, incorporating both ΔBP and BP, could potentially yield better performance outcomes.

Table 5
Performance comparison for different data balancing techniques using the optimal feature combination without pretraining (SBP).

		MAE of SBP (mmHg)	MAE of ΔSBP (mmHg)	Intra-subject correlation	Overall SBP correlation
Dataset-KSU	Unbalanced	4.35	5.51	0.50	0.91
	Balanced BP	4.20	5.33	0.48	0.92
	Balanced ΔBP	5.14*	5.24	0.42*	0.80*
Dataset-SIBET	Unbalanced	11.83	13.28	0.45	0.61
	Balanced BP	10.67*	12.82	0.51	0.72*
	Balanced ΔBP	10.62*	11.22*	0.45	0.74*
	Base-KSU	12.02	15.33	0.58*	0.66

* significantly different from algorithms with unbalanced data and no pretraining.

One notable observation was that ΔBP balancing alone did not lead to an improvement in ΔBP correlation or intra-subject correlation, as shown in Table 5 and supplementary Table 3. Further examination revealed that removing several outliers could have significantly enhanced the intra-subject correlation. These outliers were likely a result of flawed ΔBP balancing due to the choice of baseline or ΔBP combinations. The incorporation of other balancing techniques along with transfer learning proved effective in mitigating this issue, as demonstrated in Table 6 and supplementary Table 4. The best BP estimation performance for dataset-KSU is illustrated in Supplementary Figure S2.

3.3. Performance enhancement by transfer learning and frequency-domain feature adaptation

Despite the utilization of different sensors, both datasets incorporated piezoelectric materials placed beneath the mattress. Through the implementation of transfer learning, specifically with unbalanced pretraining and ΔBP balanced retraining, we achieved significant improvements in r performance, as evidenced in Table 6. The overall SBP correlation increased from 0.74 to 0.79, and the ΔSBP correlation improved from 0.45 to 0.67, representing a substantial enhancement. The best BP estimation performance for dataset-SIBET is illustrated in Supplementary Figure S3.

However, it is important to note that MAE of SBP was mainly improved by data-balancing, not transfer learning. In addition, algorithms utilizing frequency-domain base functions from dataset-KSU demonstrated similar performance, although the MAE of ΔSBP is higher. This observation suggests that there is a potential degree of equivalence between the two bed sensor systems.

It is important to acknowledge that the two piezoelectric sensors used in this study were similar. Although there were demographic differences between the two datasets, the principal base function could be transferred from one to another. However, adaptation of spectral principal components still resulted in favorable results.

Table 6
Performance using different preprocessing steps with optimal feature combinations (SBP).

Base function	Base-SIBET					Base-KSU	
Pretraining (KSU)	Unbalanced	Unbalanced	Unbalanced	Balanced BP	Balanced ΔBP	Balanced BP	Balanced ΔBP
Transfer learning	Unbalanced BP or ΔBP	Balanced BP	Balanced ΔBP	balanced BP	Balanced ΔBP	balanced BP	Balanced ΔBP
MAE of SBP estimation(mmHg)	10.56	10.28	10.32	10.04	10.92*	11.45*	9.96
MAE of ΔSBP estimation(mmHg)	13.23	12.61	11.01*	13.27	13.63	13.65	13.22
Intra-subject correlation	0.66*	0.67*	0.67*	0.67*	0.62	0.65	0.66*
Overall SBP correlation	0.74	0.75	0.79	0.77	0.69	0.72	0.78

* significantly different from the no pretraining and BP balanced algorithm with optimal feature combinations.

3.4. Comparison with previous studies

As far as we know, we were the first to report BCG-derived BP in subjects with cardiovascular dysfunctions. To make a fair comparison with previous studies, we only used results from dataset-KSU, and added calibrated results, as shown in Table 7.

Our multi-domain feature combination scheme demonstrated substantial improvement over most previous studies. Even our TD-feature-only scheme performed better, potentially due to the novel application of the EasyEnsemble data-balancing technique, which significantly improved BP estimation accuracy [52]. Although Su *et al.* reported smaller MAE, they only collected 5–6 measurements per subject [13], while we had an average of 362 measurements per subject and obtained fast-changing BP using Finapres. Therefore, differences in cohort and study design may have contributed to the variations in our results, as discussed in [59].

4. Discussion

4.1. Novelty of the study

BCG-based BP estimation technologies have gained interest due to their comfort and convenience, but limitations exist. Most of the existing methods were based on BCG measured by weighing scales, chairs, or devices worn on limbs, which were not optimal for overnight BP estimation. The established algorithms mainly utilized morphological feature extraction and pulse wave velocity calculation, while the cohorts used were primarily young and healthy. Our study addressed these limitations by employing novel piezoelectric bed sensor systems for BCG measurement, utilizing spectral and morphological features to reflect the overall BP levels. We added HFD to account for residual vibrations, significantly improving intra-subject BP fluctuation estimation. Biometrics are used to estimate healthy subject skeletomuscular properties, while calibration is necessary for in-hospital patients and older subjects. The strategic feature combination maximized the information fed into the machine learning algorithm, yielding robust results. For older and diseased patients, augmenting BCG data with other modalities may help improve performance.

Our research further revealed the substantial impact of data balancing and transfer learning on the performance of the algorithm. Studies have shown that both intra- and inter-subject variabilities in BP can affect the machine learning algorithms [53]. As a result, we conducted experiments to evaluate the effectiveness of a novel ΔBP balancing technique alongside conventional BP balancing. Remarkably, the ΔBP balancing technique exhibited good outcomes, particularly for in-hospital patients. The integration of transfer learning was instrumental in improving the accuracy of our system and capturing the underlying shared characteristics of the two distinct sensor setups. By incorporating transfer learning, we not only enhanced the overall accuracy of the algorithm but also improved its generalization capabilities. This allowed for more robust algorithm development. Consequently, our algorithm can be more readily applied to new target populations or data from similar devices.

4.2. Comparison with previous studies

Few studies have used bed-based BCG to estimate BP [13,19,26]. The main problem was that the measured force-BCG was nearly perpendicular to blood ejection from the aortic artery, which weakened the signal and complicated the correlation between BCG and BP. Acceleration-based BCG could measure BCG in the direction of blood ejection, but for a bed-sensor system, its signal was strongly influenced by the mechanical coupling of the human body and the mattress. Su *et al.* showed a high correlation between BCG amplitude and BP [13]. However, the applicability of their findings to older individuals or those with severe cardiovascular dysfunctions remains uncertain. In this study, we included such subjects and assessed the performance of the BCG-BP algorithm. Interestingly, knowledge acquired from the analysis of healthy subjects facilitated the development of the algorithm targeting diseased populations. These findings hold potential for future studies focusing on more challenging populations.

Most of the previous studies required personalized calibration. Guidoboni *et al.* built a closed-loop mathematical model for the cardiovascular system, showing the importance of age, weight distribution, and height in BCG waveform formation [19]. We demonstrated that the information provided by these features was not redundant, instead improving the accuracy of blood pressure estimation. Biometric data may help estimate personalized calibration factors for healthy subjects, leading to a calibration-free system. However, for subjects with abnormal health conditions, calibration factors need to be measured. To the best of our knowledge, we were the first to include older individuals and those with diseases in the BCG-BP study, and the validity of our

Table 7
Comparison with other BCG-BP algorithms.

Studies	Study design		Features	MAE (mmHg)		Overall correlation	
	Posture	Calibration		SBP	DBP	SBP	DBP
Our method	Supine	N	TD + FD+HFD + Bios	4.20	4.25	0.92	0.85
Our method	Supine	Y	TD + FD+HFD + Bios	3.76	3.23	0.93	0.91
Our method	Supine	N	TD	7.18	6.07	0.80	0.68
Our method	Supine	Y	TD	5.03	3.20	0.91	0.90
Su *et al.*[13]	Supine	Y	TD	1.81	2.34	0.91	0.84
Yousefian *et al.*[23]	Standing	Y	TD	8.3	6.0	0.75	0.75
Yousefian *et al.*[24]	Standing	Y	TD + PTT	7.6	5.1	0.81	0.79
Martin *et al.*[22]	Standing	Y	PTT	11.8(RMSE)	7.6(RMSE)	0.80	0.80
Kim *et al.*[18]	Standing	Y	TD	8.1(RMSE)	6.8(RMSE)	0.73	0.70

algorithm was confirmed by transfer learning across databases.

4.3. Limitations of the study

Differences in performance between cohorts may be attributed to demographics, cardiovascular conditions, bed-sensor system or protocol design. For example, lack of overnight study subject constraints may have impacted the corresponding algorithm's performance. Despite these differences, transfer learning from dataset-KSU significantly improved BP estimation performance in dataset-SIBET, suggesting similarity of the sensor systems. Future studies could benefit from side-by-side concurrent measurement and comparison.

In this study, we focused on the completeness of the information. Some redundancy remained in the final combined features. Orthogonalization or principal component analysis across multi-domains should be carried out to obtain the best feature combination. The BNN structure should be tuned accordingly.

Although the two bed-sensor systems had multiple sensors, we only used one to derive BP, which didn't utilize the PTT information. We found that respiration distorted the signal morphology, which reduced the reliability of the PTT calculation. Thus, the addition of other BCG sensors didn't improve the BP estimation accuracy. Posture recognition and the addition of wrist sensors might help.

Dataset-KSU had more physiological signals such as electrocardiogram(ECG) and SV, we kept our focus on BCG to estimate the performance of a bed-sensor system without any wearables. Another reason is that we didn't collect these signals in dataset-SIBET. In the future, multimodal signals should be collected for a more thorough comparison.

4.4. Suggestions for future work

For unobtrusive BP estimation, the information provided by a single modality was limited. With the advancement of sensor technologies, more and more vital signs could be measured without direct contact, such as capacitive electrocardiogram (cECG), remote PPG (rPPG), and magnetic induction monitoring. When multiple modalities were combined, they may complement each other, and provide better estimation results than any single signal. If enough information was contained by the measurement, a proper fusion method should be designed and the machine learning structure should be optimized accordingly.

5. Conclusion

Bed sensor systems are very convenient for sleep BP estimation. Compared to wearable devices, they operate non-obtrusively and require minimal maintenance. We found that morphological and spectral features of BCG contain non-identical information on overall BP levels, while HFD provided essential information for BP trend monitoring. For young and healthy subjects, a calibration-free BP estimation is possible. However, for older or diseased subjects, the information contained in the BCG signal is not enough to obtain a high-performance algorithm. Additional information from other modalities should be used to bring improvement. Sleep BP monitoring should be explored with the additional sleep posture recognition, which needs more sensors and guidance from the closed-loop distributed weight model.

CRediT authorship contribution statement

Xiaoman Xing: Conceptualization, Methodology, Writing – review & editing. **Huan Li:** Data curation. **Qi Chen:** Data curation. **Chenyu Jiang:** Investigation, Validation. **Wen-fei Dong:** Supervision.

Declaration of Competing Interest

The authors declare that they have no known competing financial interests or personal relationships that could have appeared to influence the work reported in this paper.

Data availability

Data will be made available on request.

Acknowledgments

This work was supported by the National Key Research and Development Program of China (2021YFC2501500, 2020YFC2003600, 2018YFC2001100), the National Natural Science Foundation of China (62001470), the Natural Science Foundation of Shandong Province, China (ZR2020QF021), and Youth Innovation Promotion Association CAS.

Appendix

Higuchi fractal dimension of BCG.

In this study, we used the Higuchi fractal dimension (HFD) of the BCG wavelet component at 2 Hz-15 Hz to measure hemodynamic complexity in the time domain, which could be simplified as time sequences $x(1)$, $x(2)$,…, $x(N)$. In this study, x represented the amplitudes of BCG at each wavelet frequency. The signal length was set to 5 s, thus N was set as 250 or 500 depending on the dataset. From the starting time, a new self-similar time series X_k^m was calculated as:

$$X_k^m : x(m), x(m+k), x(m+2k), \cdots, x\left(m + int\left[\frac{N-m}{k}\right]k\right), m = 1, 2, \cdots, k \tag{1}$$

m is the initial time; k is the time interval by counting the number of heartbeats, $k = 1,\ldots,k_{\max}$. $\mathrm{int}\{\frac{N-m}{k}\}$ is the integer part of the real number $\frac{N-m}{k}$. The length of the curve $L_m(k)$ was computed for X_k^m as

$$L_m(k) = \frac{1}{k}\left[\left(\sum_{i=1}^{int\left[\frac{N-m}{k}\right]} |x(m+ik) - x(m+(i-1)k)|\right)\frac{N-1}{int\left[\frac{N-m}{k}\right]k}\right. \tag{2}$$

N is the length of the original time series X, and $\frac{N-1}{int\left[\frac{N-m}{k}\right]k}$ is a normalization factor. $L_m(k)$ was averaged for all m. The mean value of the curve length $L(k)$ is defined as

$$L(k) = \frac{1}{k}\sum_{m=1}^{k} L_m(k) \tag{3}$$

An array of $L(k)$ was obtained and HFD was estimated as the slope of the linear best fit from the plot of $\ln(L(k))$ versus $\ln(1/k)$. In this study, k_{max} was set as 100 for dataset-KSU and 50 for dataset-SIBET due to sampling frequency differences. For dataset-KSU, HFDs at different wavelet frequencies were highly correlated. Thus, we chose the HFD with the highest wavelet amplitude for dataset-KSU. For dataset-SIBET, correlation analysis showed two major HFD components. Principal component decomposition was carried out and we chose the two most important components as HFD features.

Declaration of generative AI and AI-assisted technologies in the writing process.

During the preparation of this work, the author(s) utilized ChatGPT 3.5 to enhance the quality of the language. Following the utilization of this service, the authors thoroughly reviewed and edited the content as necessary, assuming full responsibility for the publication's content.

Appendix A. Supplementary data

Supplementary data to this article can be found online at https://doi.org/10.1016/j.bspc.2023.105479.

References

[1] R.C. Hermida, D.E. Ayala, M.H. Smolensky, J.R. Fernández, A. Mojón, F. Portaluppi, Sleep-time blood pressure: Unique sensitive prognostic marker of vascular risk and therapeutic target for prevention, Sleep Medicine Reviews 33 (2017) 17–27.

[2] R.M. Bruno, S. Taddei, Asleep blood pressure: a target for cardiovascular event reduction? European Heart Journal 39 (2018) 4172–4174.

[3] R.C. Hermida, J.J. Crespo, A. Otero, M. Domínguez-Sardiña, A. Moyá, M.T. Ríos, M. C. Castiñeira, P.A. Callejas, L. Pousa, E. Sineiro, J.L. Salgado, C. Durán, J. J. Sánchez, J.R. Fernández, A. Mojón, D.E. Ayala, Asleep blood pressure: Significant prognostic marker of vascular risk and therapeutic target for prevention, European Heart Journal 39 (2018) 4159–4171.

[4] N. Staplin, A. de la Sierra, L.M. Ruilope, J.R. Emberson, E. Vinyoles, M. Gorostidi, G. Ruiz-Hurtado, J. Segura, C. Baigent, B. Williams, Relationship between clinic and ambulatory blood pressure and mortality: An observational cohort study in 59 124 patients, Lancet 401 (2023) 2041–2050.

[5] T. Ohkubo, Y. Imai, I. Tsuji, K. Nagai, N. Watanabe, N. Minami, J. Kato, N. Kikuchi, A. Nishiyama, A. Aihara, M. Sekino, H. Satoh, S. Hisamichi, Relation between nocturnal decline in blood pressure and mortality: The ohasama study, American Journal of Hypertension 10 (1997) 1201–1207.

[6] E. Tasali, B. Mokhlesi, E. Van Cauter, Obstructive sleep apnea and type 2 diabetes: Interacting epidemics, Chest 133 (2008) 496–506.

[7] J.-L. Pepin, A.-L. Borel, R. Tamisier, J.-P. Baguet, P. Levy, Y. Dauvilliers, Hypertension and sleep: Overview of a tight relationship, Sleep Medicine Reviews 18 (6) (2014) 509–519.

[8] N.M. Punjabi, E. Shahar, S. Redline, D.J. Gottlieb, R. Givelber, H.E. Resnick, Sleep-disordered breathing, glucose intolerance, and insulin resistance: The sleep heart health study, American Journal of Epidemiology 160 (2004) 521–530.

[9] K.L. Knutson, K. Spiegel, P. Penev, E. Van Cauter, The metabolic consequences of sleep deprivation, Sleep Medicine Reviews 11 (2007) 163–178.

[10] B. Silke, D. McAuley, Accuracy and precision of blood pressure determination with the finapres: An overview using re-sampling statistics, Journal of Human Hypertension 12 (1998) 403–409.

[11] T. Komori, K. Eguchi, S. Hoshide, B. Williams, K. Kario, Comparison of wrist-type and arm-type 24-h blood pressure monitoring devices for ambulatory use, Blood Pressure Monitoring 18 (2013) 57–62.

[12] R. Mukkamala, J.-O. Hahn, A. Chandrasekhar, in: Photoplethysmography, Elsevier, 2022, pp. 359–400.

[13] B.Y. Su, M. Enayati, K.C. Ho, M. Skubic, L. Despins, J. Keller, M. Popescu, G. Guidoboni, M. Rantz, Monitoring the relative blood pressure using a hydraulic bed sensor system, I.E.E.E. Transactions on Bio-Medical Engineering 66 (2019) 740–748.

[14] K. Tavakolian, O. Inan, J.-O. Hahn, M. Di Rienzo, Editorial: Cardiac vibration signals: Old techniques, New Tricks, and Applications, Frontiers in Physiology 13 (2022) 931362.

[15] H. Wang, L. Wang, N. Sun, Y. Yao, L. Hao, L. Xu, S.E. Greenwald, Quantitative comparison of the performance of piezoresistive piezoelectric, acceleration, and optical pulse wave sensors, Front Physiol 10 (2019) 1563.

[16] P. Yousefian, S. Shin, A.S. Mousavi, C.-S. Kim, B. Finegan, M.S. McMurtry, R. Mukkamala, D.-G. Jang, U. Kwon, Y.H. Kim, J.-O. Hahn, Physiological association between limb ballistocardiogram and arterial blood pressure waveforms: A mathematical model-based analysis, Scientific Reports 9 (2019) 5146.

[17] C.-S. Kim, S.L. Ober, M.S. McMurtry, B.A. Finegan, O.T. Inan, R. Mukkamala, J.-O. Hahn, Ballistocardiogram: Mechanism and potential for unobtrusive cardiovascular health monitoring, Scientific Reports 6 (2016) 31297.

[18] C.-S. Kim, A.M. Carek, O.T. Inan, R. Mukkamala, J.-O. Hahn, Ballistocardiogram-based approach to cuffless blood pressure monitoring: Proof of concept and potential challenges, I.E.E.E. Transactions on Bio-Medical Engineering 65 (11) (2018) 2384–2391.

[19] G. Guidoboni, L. Sala, M. Enayati, R. Sacco, M. Szopos, J.M. Keller, M. Popescu, L. Despins, V.H. Huxley, M. Skubic, Cardiovascular function and ballistocardiogram: A relationship interpreted via mathematical modeling, IEEE Transactions on Biomedical Engineering 66 (10) (2019) 2906–2917.

[20] I. Sadek, J. Biswas, B. Abdulrazak, Ballistocardiogram signal processing: A review, Health Inf Sci Syst 7 (2019) 10.

[21] O.T. Inan, P.-F. Migeotte, K.-S. Park, M. Etemadi, K. Tavakolian, R. Casanella, J. Zanetti, J. Tank, I. Funtova, G.K. Prisk, M. Di Rienzo, Ballistocardiography and seismocardiography: A review of recent advances, IEEE Journal of Biomedical and Health Informatics 19 (4) (2015) 1414–1427.

[22] S.L.O. Martin, A.M. Carek, C.-S. Kim, H. Ashouri, O.T. Inan, J.-O. Hahn, R. Mukkamala, Weighing scale-based pulse transit time is a superior marker of blood pressure than conventional pulse arrival time, Scientific Reports 6 (2016) 39273.

[23] P. Yousefian, S. Shin, A. Mousavi, C.-S. Kim, R. Mukkamala, D.-G. Jang, B.-H. Ko, J. Lee, U.K. Kwon, Y.H. Kim, J.-O. Hahn, Data mining investigation of the association between a limb ballistocardiogram and blood pressure, Physiological Measurement 39 (7) (2018) 075009.

[24] P. Yousefian, S. Shin, A. Mousavi, C.-S. Kim, R. Mukkamala, D.-G. Jang, B.-H. Ko, J. Lee, U.K. Kwon, Y.H. Kim, J.-O. Hahn, The potential of wearable limb ballistocardiogram in blood pressure monitoring via pulse transit time, Scientific Reports 9 (2019) 10666.

[25] P. Yousefian, S. Shin, A. Mousavi, A. Tivay, C.-S. Kim, R. Mukkamala, D.-G. Jang, B.-H. Ko, J. Lee, U.-K. Kwon, Y. Kim, J.-O. Hahn, Pulse transit time-pulse wave analysis fusion based on wearable wrist ballistocardiogram for cuff-less blood pressure trend tracking, IEEE Access 8 (2020) 1.

[26] C. Carlson, V.R. Turpin, A. Suliman, C. Ade, S. Warren, D.E. Thompson, Bed-based ballistocardiography: dataset and ability to track cardiovascular parameters, Sensors (Basel) 21 (2020).

[27] Z. Chen W. Chen H. Hee P. Zhao M. Yu W. Chen Ballistocardiography based on optical fiber sensors, 2017.

[28] X. Yu, W. Neu, P. Vetter, L.C. Bollheimer, S. Leonhardt, D. Teichmann, C.H. Antink, A multi-modal sensor for a bed-integrated unobtrusive vital signs sensing array, IEEE Transactions on Biomedical Circuits and Systems 13 (2019) 529–539.

[29] O. Linschmann, S. Leonhardt, A. Vehkaoja, C. Hoog Antink, Estimation of the respiratory rate from ballistocardiograms using the hilbert transform, BioMedical Engineering OnLine 21 (2022).

[30] M.D. Zink, C. Brüser, P. Winnersbach, A. Napp, S. Leonhardt, N. Marx, P. Schauerte, K. Mischke, Heartbeat cycle length detection by a ballistocardiographic sensor in atrial fibrillation and sinus rhythm, Biomed Research International 2015 (2015) 840356.

[31] M. Zhang, L. Qiu, Y. Chen, S. Yang, Z. Zhang, L. Wang, A Conv -Transformer network for heart rate estimation using ballistocardiographic signals, Biomedical Signal Processing and Control 80 (2023) 104302.

[32] Y. Yao, S. Shin, A. Mousavi, C.-S. Kim, L. Xu, R. Mukkamala, J.-O. Hahn, Unobtrusive estimation of cardiovascular parameters with limb ballistocardiography, Sensors (Basel) 19 (13) (2019) 2922.

[33] J.H. Shin, K.M. Lee, K.S. Park, Non-constrained monitoring of systolic blood pressure on a weighing scale, Physiological Measurement 30 (2009) 679.

[34] J.H. Shin, K.S. Park, HRV analysis and blood pressure monitoring on weighing scale using BCG, Annu Int Conf IEEE Eng Med Biol Soc 2012 (2012) 3789–3792.

[35] D.D. He, E.S. Winokur, C.G. Sodini, An ear-worn vital signs monitor, I.E.E.E. Transactions on Bio-Medical Engineering 62 (2015) 2547–2552.

[36] J. Alametsä, J. Viik, J. Alakare, A. Värri, A. Palomäki, Ballistocardiography in sitting and horizontal positions, Physiological Measurement 29 (2008) 1071–1087.

[37] A.Q. Javaid, A.D. Wiens, N.F. Fesmire, M.A. Weitnauer, O.T. Inan, Quantifying and reducing posture-dependent distortion in ballistocardiogram measurements, IEEE Journal of Biomedical and Health Informatics 19 (2015) 1549–1556.

[38] S. Shin, A. Mousavi, S. Lyle, E. Jang, P. Yousefian, R. Mukkamala, D.-G. Jang, U. Kwon, Y. Kim, J.-O. Hahn, Posture-dependent variability in wrist ballistocardiogram-photoplethysmogram pulse transit time: Implication to cuff-less blood pressure tracking, IEEE Transactions on Biomedical Engineering (2021) 1.

[39] D. Shao, F. Tsow, C. Liu, Y. Yang, N. Tao, Simultaneous monitoring of ballistocardiogram and photoplethysmogram using a camera, I.E.E.E. Transactions on Bio-Medical Engineering 64 (2017) 1003–1010.

[40] E. Pinheiro, O. Postolache, P. Girão, Theory and developments in an unobtrusive cardiovascular system representation: ballistocardiography, Open Biomedical Engineering Journal 4 (1) (2010) 201–216.
[41] J. Hashimoto, K. Chonan, Y. Aoki, T. Nishimura, T. Ohkubo, A. Hozawa, M. Suzuki, M. Matsubara, M. Michimata, T. Araki, Y. Imai, Pulse wave velocity and the second derivative of the finger photoplethysmogram in treated hypertensive patients: Their relationship and associating factors, Journal of Hypertension 20 (2002) 2415–2422.
[42] D. Brillante, A. O'Sullivan, L. Howes, Arterial stiffness indices in healthy volunteers using non-invasive digital photoplethysmography, Blood pressure 17 (2008) 116–123.
[43] S. Dehghanojamahalleh, M. Kaya, Sex-related differences in photoplethysmography signals measured from finger and toe, IEEE J Transl Eng Health Med 7 (2019) 1900607.
[44] A. Suliman, M.R. Mowla, A. Alivar, C. Carlson, P. Prakash, B. Natarajan, S. Warren, D.E. Thompson, Effects of ballistocardiogram peak detection jitters on the quality of heart rate variability features: A simulation-based case study in the context of sleep staging, Sensors (Basel) 23 (2023).
[45] C. Carlson, A. Suliman, P. Prakash, D. Thompson, W. Shangxian, B. Natarajan, S. Warren, Bed-based instrumentation for unobtrusive sleep quality assessment in severely disabled autistic children, Annu Int Conf IEEE Eng Med Biol Soc 2016 (2016) 4909–4912.
[46] D.P. Garg, M.A. Ross, Vertical mode human body vibration transmissibility, IEEE Transactions on Systems, Man, and Cybernetics SMC-6 (2) (1976) 102–112.
[47] Y. Yao, M.M.H. Shandhi, J.-O. Hahn, O.T. Inan, R. Mukkamala, L. Xu, What filter passband should be applied to the ballistocardiogram? Biomedical Signal Processing and Control 85 (2023) 104909.
[48] L. Guohua, W. Jianqi, Y. Yu, J. Xijing, Study of the ballistocardiogram signal in life detection system based on radar, Annu Int Conf IEEE Eng Med Biol Soc 2007 (2007) 2191–2194.
[49] J.N. Edson, ROBERT Dickes, G.H. Flamm, MICHAEL Tobin, Higher frequency phenomena in the normal ballistocardiogram, Circulation Research 1 (5) (1953) 405–409.
[50] M.D. Zink, C. Brüser, B.O. Stüben, A. Napp, R. Stöhr, S. Leonhardt, N. Marx, K. Mischke, J.B. Schulz, J. Schiefer, Unobtrusive nocturnal heartbeat monitoring by a ballistocardiographic sensor in patients with sleep disordered breathing, Scientific Reports 7 (2017) 13175.
[51] O. Linschmann, S. Leonhardt, A. Vehkaoja, C. Hoog Antink, Estimation of the respiratory rate from ballistocardiograms using the hilbert transform, BioMedical Engineering OnLine 21 (2022) 54.
[52] T.Y. Liu, EasyEnsemble and feature selection for imbalance data sets, 2009 international joint conference on bioinformatics, Systems Biology and Intelligent Computing (2009) 517–520.
[53] R.C. Moore, D.P.W. Ellis, E. Fonseca, S. Hershey, A. Jansen, M. Plakal, Dataset balancing can hurt model performance, ICASSP 2023 - 2023 IEEE international conference on acoustics, Speech and Signal Processing (ICASSP) (2023) 1–5.
[54] V. Fleischhauer, A. Feldheiser, S. Zaunseder, Beat-to-beat blood pressure estimation by photoplethysmography and its interpretation, Sensors 22 (2022) 7037.
[55] W. Wang, P. Mohseni, K.L. Kilgore, L. Najafizadeh, Cuff-less blood pressure estimation from photoplethysmography via visibility graph and transfer learning, IEEE Journal of Biomedical and Health Informatics 26 (2022) 2075–2085.
[56] F. Zhuang, Z. Qi, K. Duan, D. Xi, Y. Zhu, H. Zhu, H. Xiong, Q. He, A comprehensive survey on transfer learning, Proceedings of the IEEE 109 (2021) 43–76.
[57] J. Leitner, P.-H. Chiang, S. Dey, Personalized blood pressure estimation using photoplethysmography: A transfer learning approach, IEEE Journal of Biomedical and Health Informatics 26 (1) (2022) 218–228.
[58] Y. Yao, Z. Ghasemi, M.M.H. Shandhi, H. Ashouri, L. Xu, R. Mukkamala, O.T. Inan, J.O. Hahn, Mitigation of instrument-dependent variability in ballistocardiogram morphology: Case study on force plate and customized weighing scale, IEEE Journal of Biomedical and Health Informatics 24 (2020) 69–78.
[59] T.L. Bothe, A. Patzak, N. Pilz, The B-Score is a novel metric for measuring the true performance of blood pressure estimation models, Scientific Reports 12 (2022) 12173.